THE JOURNAL OF BIOLOGICAL CHEMISTRY VOL. 287, NO. 20, pp. 16187–16198, May 11, 2012

Mouse Betaine-Homocysteine *S*-Methyltransferase Deficiency Reduces Body Fat via Increasing Energy Expenditure and Impairing Lipid Synthesis and Enhancing Glucose Oxidation in White Adipose Tissue*

Received for publication, September 11, 2011, and in revised February 21, 2012 Published, JBC Papers in Press, February 23, 2012, DOI 10.1074/jbc.M111.303255

Ya-Wen Teng[‡], **Jessica M. Ellis**[‡§], **Rosalind A. Coleman**[‡], **and Steven H. Zeisel**[‡¶1]

From the [‡]*Department of Nutrition, School of Public Health, University of North Carolina, Chapel Hill, North Carolina 27599, the* [§]*Department of Biological Chemistry, The Johns Hopkins University, Baltimore, Maryland 21205, and the* [¶]*Nutrition Research Institute, University of North Carolina at Chapel Hill, Kannapolis, North Carolina 28081*

Background: Mice with the gene encoding betaine-homocysteine *S*-methyltransferase deleted ($Bhmt^{-/-}$) have absent hepatic BHMT activity and reduced fat mass.
Results: $Bhmt^{-/-}$ mice have increased energy expenditure, reduced fat synthesis, and enhanced glucose oxidation in white adipose tissue.
Conclusion: BHMT plays a role in energy homeostasis.
Significance: Liver BHMT activity affects adipose tissue metabolism.

Betaine-homocysteine *S*-methyltransferase (BHMT) catalyzes the synthesis of methionine from homocysteine. In our initial report, we observed a reduced body weight in $Bhmt^{-/-}$ mice. We initiated this study to investigate the potential role of BHMT in energy metabolism. Compared with the controls ($Bhmt^{+/+}$), $Bhmt^{-/-}$ mice had less fat mass, smaller adipocytes, and better glucose and insulin sensitivities. Compared with the controls, $Bhmt^{-/-}$ mice had increased energy expenditure, with no changes in food intake, fat uptake or absorption, or in locomotor activity. The reduced adiposity in $Bhmt^{-/-}$ mice was not due to hyperthermogenesis. $Bhmt^{-/-}$ mice failed to maintain a normal body temperature upon cold exposure because of limited fuel supplies. *In vivo* and *ex vivo* tests showed that $Bhmt^{-/-}$ mice had normal lipolytic function. The rate of ^{14}C-labeled fatty acid incorporated into [^{14}C]triacylglycerol was the same in $Bhmt^{+/+}$ and $Bhmt^{-/-}$ gonadal fat depots (GWAT), but it was 62% lower in $Bhmt^{-/-}$ inguinal fat depots (IWAT) compared with that of $Bhmt^{+/+}$ mice. The rate of ^{14}C-labeled fatty acid oxidation was the same in both GWAT and IWAT from $Bhmt^{+/+}$ and $Bhmt^{-/-}$ mice. At basal level, $Bhmt^{-/-}$ GWAT had the same [^{14}C]glucose oxidation as did the controls. When stimulated with insulin, $Bhmt^{-/-}$ GWAT oxidized 2.4-fold more glucose than did the controls. Compared with the controls, the rate of [^{14}C]glucose oxidation was 2.4- and 1.8-fold higher, respectively, in $Bhmt^{-/-}$ IWAT without or with insulin stimulus. Our results show for the first time a role for BHMT in energy homeostasis.

Betaine-homocysteine *S*-methyltransferase (BHMT)[2] is an enzyme predominantly found in the liver in rodents (1), and it plays an essential role in regulating one-carbon metabolism. BHMT catalyzes the formation of the amino acid methionine from homocysteine using the choline metabolite betaine as the methyl donor. BHMT deficiency leads to elevated betaine and homocysteine concentrations and reduced choline concentration (2). BHMT also influences hepatic lipid accumulation via altering phosphatidylcholine (PtdCho) concentration. BHMT exerts this effect through two mechanisms. First, choline, the precursor of betaine, can alternatively be used to make PtdCho via the Kennedy pathway. Second, methionine, the end product of BHMT, is the precursor of *S*-adenosylmethionine, which is required for the synthesis of PtdCho from phosphatidylethanolamine by the enzyme phosphatidylethanolamine methyltransferase. BHMT overexpression increases PtdCho synthesis, leading to reduced hepatic lipid accumulation (3), whereas BHMT deficiency leads to fatty liver (2). Although the role of BHMT in hepatic lipid metabolism has been elucidated, there is no previous evidence that BHMT plays a role in whole body energy metabolism and adiposity.

We observed that *Bhmt*-deficient ($Bhmt^{-/-}$) mice had a lower body weight from 5 to 9 weeks of age compared with wild type littermates (2). Magnetic resonance image (MRI) analysis and dissection of adipose fat depots revealed that the reduced

* This work was supported, in whole or in part, by National Institutes of Health Grants DK55865 and DK56350 (to S. H. Z.), DK59935 and DK56598 (to R. A. C.), and Predoctoral Training Grant T32-HL069768 (to J. M. E.). This work was also supported by a McNeil Nutritionals predoctoral fellowship (to Y.-W. T.), a dissertation completion fellowship from the University of North Carolina at Chapel Hill (to Y.-W. T.), and a predoctoral fellowship from the American Heart Association Mid-Atlantic Division (to J. M. E.).

[1] To whom correspondence should be addressed: 500 Laureate Way, Kannapolis, NC 28081. Tel.: 704-250-5003; Fax: 704-250-5001; E-mail: steven_zeisel@unc.edu.

[2] The abbreviations used are: BHMT, betaine-homocysteine *S*-methyltransferase; PtdCho, phosphatidylcholine; NEFA, nonesterified fatty acid; TAG, triacylglycerol; ASM, acid-soluble metabolites; GWAT, gonadal white adipose tissue; IWAT, inguinal white adipose tissue; BAT, brown adipose tissue; RER, respiratory exchange ratio; FGF21, fibroblast growth factor 21; T_4, thyroxine; T_3, triiodothyronine; WAT, white adipose tissue; FA, fatty acid; BW, body weight.

body weight observed in *Bhmt*$^{-/-}$ mice was due to reduced fat depots. These results suggested that *Bhmt*-deficient mice might have problems with energy metabolism. This study aims to examine the metabolic perturbations that lead to the reduced adiposity observed in *Bhmt*$^{-/-}$ mice. Homeostasis of energy stores is regulated by mechanisms, including modulation of metabolic rate and thermogenesis, control of metabolite fluxes among various organs, and modulation of fuel synthesis and use within tissues. We present evidence that *Bhmt*$^{-/-}$ mice have reduced adiposity due to increased whole body metabolic rate, impaired triglyceride synthesis, and enhanced glucose oxidation in white adipose tissue (WAT).

EXPERIMENTAL PROCEDURES

Generation and Maintenance of Mice—The strategy used to generate *Bhmt*$^{-/-}$ mice was as described previously (2). *Bhmt*$^{-/-}$ mice and their wild type littermates were of a C57Bl/6×sv129 genetic background and were continuously backcrossed to C57Bl/6 mice. Generations F3 to F5 were used in this study. The animals were kept in a temperature-controlled environment at 24 °C and exposed to a 12-h light and dark cycle. All animals received AIN-76A pelleted diet with 1.1 g/kg choline chloride (Dyets, Bethlehem, PA). The Institutional Animal Care and Use Committee of the University of North Carolina at Chapel Hill approved all experimental protocols.

BHMT Western Blot—Mice were anesthetized by inhalation of isoflurane (Hospira, Lake Forest, IL). Tissues were harvested, snap-frozen, pulverized under liquid nitrogen, and stored at −80 °C until used. Western blot analysis was performed in liver and adipose homogenates as described previously (4).

Metabolic Studies—Body composition was determined in 7- and 14-week-old mice by MRI (EchoMRI-100, Echo Medical Systems, LLC, Houston). Core temperature was measured in 7-week-old mice using a rectal probe thermometer (Thermalert TH-5, Physitemp, Clifton, NJ). Food intake, oxygen consumption (VO_2), carbon dioxide release (VCO_2), and locomotor activity were measured every 27 min from individually housed mice (7-week-old) using indirect calorimetry (TSE Systems, Germany) with an airflow of 0.25 liter/min. Locomotor activity was measured using infrared technology as the counts of three-dimensional beam breaking (*X* total, *Y* total, and *Z* total). Respiratory exchange ratio (RER) was calculated as VCO_2/VO_2. Mice were acclimated to the chambers for 24 h, and data were collected during the following 24 h. Stool samples were collected, and TAG was extracted using the Folch method (5) and measured colorimetrically (Sigma). For cold tolerance tests, 7-week-old mice were fasted for 4 h before being exposed to cold (4 °C) without food or bedding. Core temperature was measured at base line and every 15 min. Mice were removed from the cold room when body temperature dropped below 28 °C.

Biochemical Assays—An oral fat load test was performed by gavaging 7-week-old mice with 10 μl/g BW olive oil after an overnight fast. Blood was collected retroorbitally at base line, 1, 2, 4, and 6 h, and plasma TAG was measured with a colorimetric assay (Sigma). Glucose and insulin tolerance tests were performed by intraperitoneally injecting either glucose (2.5 g/kg BW) or human insulin (1 unit/kg BW, Novo Nordisk Inc., Princeton, NJ) to 7-week-old mice after a 6- or 4-h fast, respectively. Blood glucose was measured at base line, 15, 30, 60, and 120 min by tail nick using a calibrated glucometer (One Touch Ultra, LifeScan, Inc., Milpitas, CA).

Plasma Metabolites—Plasma insulin (Ultra-sensitive Mouse Insulin ELISA kit, Crystal Chem Inc., Downers Grove, IL), total thyroxine (T_4), total triiodothyronine (T_3) (Alpha Diagnostic International, San Antonio, TX), and growth hormone (Millipore) levels were determined using commercially available ELISA kits according to the manufacturers' protocols. Plasma fibroblast growth factor 21 (FGF21) (Phoenix Pharmaceuticals Inc., Burlingame, CA) and glucagon (Millipore) were determined using RIA kits according to the manufacturers' protocols. Plasma creatine kinase was measured using an automatic chemical analyzer (Johnson and Johnson VT250, Rochester, NY) at the Animal Clinical Chemistry and Gene Expression Facility, University of North Carolina, Chapel Hill. Plasma TAG, glycerol (Sigma), and nonesterified fatty acids (NEFA) (Wako, Richmond, VA) were measured colorimetrically per the manufacturers' instructions. Plasma glucose was measured using a calibrated glucometer (One Touch Ultra).

Tissue Metabolites—Hepatic free glucose and glycogen were measured using an adopted acid hydrolysis method (6). Liver was collected from mice after a 4-h fast. Briefly, 40 mg of pulverized liver was homogenized in 1 ml of 1 N HCl. Half of the homogenate was neutralized with 0.5 ml of 1 M NaOH (nonhydrolyzed group). The other half was incubated at 95 °C for 90 min before being neutralized with NaOH (hydrolyzed group). Glucosyl units released in both groups were measured using a colorimetrical glucose kit (Wako). The nonhydrolyzed group represented the free glucose measurement, while the difference between the hydrolyzed and the nonhydrolyzed groups represented the glycogen measurement. For bile acids and steroids, liver and gonadal fat pads were collected from 5-week-old mice after a 4-h fast. Tissues were sent to Metabolon (Research Triangle Park, NC), where the metabolites were measured using gas chromatography/mass spectrometry (GC/MS) and liquid chromatography/mass spectrometry (LC/MS) platforms as described previously (7–10). Data were extracted and analyzed by Metabolon (7–10). Briefly, raw data counts for each compound were corrected for variation resulting from instrument inter-day tuning differences and then rescaled to median equal 1. Data were expressed as fold change relative to wild type controls.

Reverse Transcription-PCR—Total RNA was isolated from tissue using RNeasy mini kit (Qiagen, Valencia, CA), and cDNA was synthesized using a high capacity cDNA reverse transcription kit (Applied Biosystems, Carlsbad, CA). cDNA was amplified by real time PCR using SsoFast EvaGreen Supermix (Bio-Rad) with primers specific to each gene of interest. Results were normalized to the housekeeping genes and calculated relative to the controls by the $2^{-\Delta\Delta CT}$ method.

Lipolysis—For *in vivo* lipolysis, mice were injected intraperitoneally with lipolytic stimuli (10 mg isoproterenol/1 kg BW or 1 mg CL316243/1 kg BW) (Sigma). Plasma was collected retroorbitally at base line and 1.5 h after injection. Plasma glycerol (Sigma) and NEFA (Wako) were measured colorimetrically, and glucose was measured using a glucometer (One Touch

Ultra). Gonadal and inguinal adipose explants were used for *ex vivo* lipolysis measurement as described previously (11, 12). Briefly, pieces of fat explants (20 mg) were incubated in 0.5 ml of Krebs Ringer Buffer (KRB) (12 mM HEPES, 121 mM NaCl, 4.9 mM KCl, 1.2 mM $MgSO_4$, and 0.33 mM $CaCl_2$) supplemented with 3.5% fatty acid-free bovine serum albumin (FFF-BSA) and 0.1% glucose with or without 10 μM isoproterenol at 37 °C. Twenty five μl of buffer was collected at various time points to measure the release of glycerol colorimetrically (Sigma).

Adipocyte Isolation—Mature adipocytes were isolated from gonadal or inguinal fat depots from 12–16 week-old mice and used for incorporation and oxidation studies (13). Briefly, gonadal or inguinal fat depots were removed under sterile conditions, minced, and incubated at 37 °C with shaking for 1 h in KRB supplemented with 1% FFF-BSA, 2.5 mM glucose, and 200 nM adenosine, containing 1 mg/ml collagenase I. The digested tissues were filtered through a sterile 250-μm mesh and washed three times with supplemented KRB. Adipocytes were diluted with supplemented KRB to reach 10% (by volume) adipocyte solution and were maintained for 30 min in a polypropylene tube before the start of the assay. Because of the small fat mass in *Bhmt*$^{-/-}$ mice, the same fat depots from two *Bhmt*$^{-/-}$ mice were pooled together to get enough adipocytes per sample.

Fatty Acid Incorporation and Oxidation—For fatty acid incorporation into TAG, 500 μl of 10% adipocyte solution were incubated with a 125-μl reaction mixture containing 15 μM [1-^{14}C]oleate (50 μCi/500 μl; PerkinElmer Life Sciences) and 200 μM unlabeled oleate complexed to BSA for 2 h at 37 °C. [^{14}C]TAG was extracted (14), isolated by thin layer chromatography, and detected and quantified with a Bioscan AR2000 Image System (Bioscan Inc., Washington, D. C.). The chromatoplate was developed in chloroform/methanol/ammonium hydroxide (65:25:4; v/v/v) to 8 cm from the top. After the residual solvents evaporated, the plate was rerun in heptane/isopropyl ether/acetic acid (60:40:4; v/v/v) to the top of the plate. For oxidation, 250 μl of 10% adipocytes solution were incubated with a 125-μl reaction mixture containing either 15 μM [1-^{14}C]oleate and 200 μM unlabeled oleate or 4 μM [^{14}C]glucose (50 μCi/500 μl; PerkinElmer Life Sciences) and 4 mM unlabeled glucose (in KRB) for 1.5 h at 37 °C. The reaction mixture was incubated in a 13-ml polypropylene tube that contained a center well filled with folded filter paper. The tube was sealed with a rubber stopper. After 1.5 h of incubation, the reaction mixture was acidified with 150 μl of 70% perchloric acid, and 300 μl of 1 M NaOH was added to the center well. The sealed tubes were incubated at RT for an additional 45 min. The center well (containing [^{14}C]CO_2 trapped by base) was then collected and placed into scintillation fluid (ScintiSafe 30% Mixture, Fisher) and counted. The acidified reaction mixture (~400 μl) was incubated overnight at 4 °C with 200 μl of 20% BSA. The mixture was centrifuged at 13,200 rpm for 20 min, and an aliquot of the supernatant was counted to determine ^{14}C-labeled acid-soluble metabolites (ASM). [^{14}C]CO_2 represents complete fatty acid or glucose oxidation, and ^{14}C-labeled ASM represents incomplete fatty acid oxidation. For some experiments, 0.01 unit of insulin (Novo Nordisk Inc., Princeton, NJ) was added. For hepatic FA oxidation experiments, fresh liver was excised, minced, and homogenated in a buffer (250 mM sucrose, 1 mM EDTA, 10 mM Tris-HCl, 2 mM ATP) to reach a 1:50 dilution. Forty μl of liver homogenate was used to measure FA oxidation as described above.

Tissue Histology—Adipose tissues were collected from 7- and 12-week-old mice and fixed in 4% paraformaldehyde in 0.1 M phosphate buffer for 24 h. Tissues were processed, paraffin-embedded, sectioned at 5 μm, and stained with hematoxylin and eosin as described previously (15). For adipocyte size analysis, three images (×200) per sample were taken, and the average adipocyte cell areas were analyzed using AxioVision 4.8 software (Zeiss).

Betaine Supplementation Study—7-Week-old *Bhmt*$^{+/+}$ mice were fed either 0 or 5% betaine (Sigma)-supplemented water for 2 weeks. Livers were collected for the measurement of *Fgf21* expression as described above.

Statistics—Statistical differences were determined using analysis of variance, Tukey-Kramer HSD, and Student's *t* test (JMP Version 6.0; SAS Institute, Cary, NC) and reported as means ± S.E. For the indirect calorimetry data analysis, the total area under the curve was calculated per measure per mouse using SAS. Statistical differences between the groups were determined using Student's *t* test (for mean comparison) and Mann-Whitney test (for median comparison).

RESULTS

BHMT Deficiency Resulted in Reduced Fat Mass and Smaller Adipocytes—We previously reported that *Bhmt*$^{-/-}$ mice gained less body weight between 5 and 9 weeks of age than did their wild type littermates ($p < 0.05$) (2). To determine whether the reduced weight gain of *Bhmt*$^{-/-}$ mice was associated with reduced fat or lean mass, we measured body composition of these mice using MRI scan analysis. *Bhmt*$^{-/-}$ mice had 20 and 30% less fat mass than did *Bhmt*$^{+/+}$ mice at 7 and 14 weeks of age, respectively ($p < 0.05$), with no significant difference in lean mass (Fig. 1*A*). The difference in fat mass was confirmed by collecting the individual fat pads. The two major white adipose tissues (WAT), gonadal (GWAT) and inguinal (IWAT), of *Bhmt*$^{-/-}$ mice were significantly smaller than those of *Bhmt*$^{+/+}$ mice at all ages (Fig. 1*B*). The disparity in fat mass was exacerbated as mice aged, such that by 48 weeks of age, *Bhmt*$^{-/-}$ mice had a fat mass that was 41% that of *Bhmt*$^{+/+}$ mice. To determine whether the reduced fat mass in *Bhmt*$^{-/-}$ mice was due to fewer fat cells and/or smaller fat cells, the sizes of individual adipocytes in GWAT and IWAT of *Bhmt*$^{+/+}$ and *Bhmt*$^{-/-}$ mice were analyzed. Histological images showed that both GWAT and IWAT from *Bhmt*$^{-/-}$ mice contained a larger number of smaller adipocytes (Fig. 1*C*). We observed a 43% reduction in adipocyte size in GWAT in both 7- and 12-week-old *Bhmt*$^{-/-}$ mice compared with those of *Bhmt*$^{+/+}$ mice ($p < 0.05$) (Fig. 1*D*). We observed a 69% ($p < 0.05$) and an 80% ($p < 0.001$) reduction in adipocyte size in IWAT in 7- and 12-week old *Bhmt*$^{-/-}$ mice, respectively, compared with those of *Bhmt*$^{+/+}$ mice (Fig. 1*D*). These data suggested that *Bhmt*$^{-/-}$ mice likely had normal adipocyte differentiation and that the *Bhmt*$^{-/-}$ adipocytes either stored less and/or used more lipids than did *Bhmt*$^{+/+}$ adipocytes. *Bhmt* is predominantly expressed in rodent liver. Western blotting confirmed that BHMT protein was specific to the liver and was absent in the

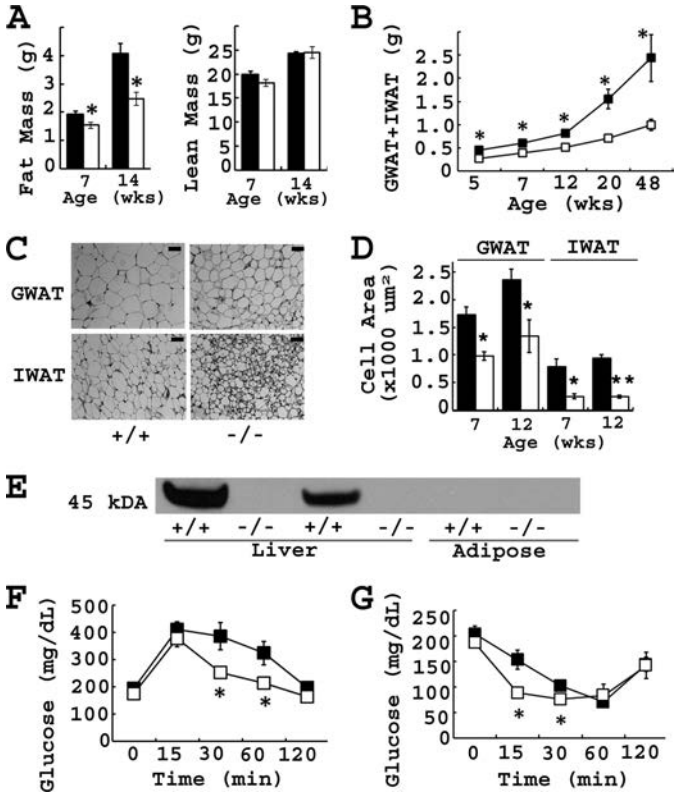

FIGURE 1. ***Bhmt*$^{-/-}$ mice had reduced adiposity and better insulin and glucose sensitivities.** *A,* body mass was measured in 7- and 14-week-old *Bhmt*$^{+/+}$ (*black bar*) and *Bhmt*$^{-/-}$ (*white bar*) mice using magnetic resonance images. *, $p < 0.05$, different from *Bhmt*$^{+/+}$ mice by Student's *t* test; $n = 12$ and 6 per group for 7- and 14-week-old mice respectively. *B,* two major fat pads, GWAT and IWAT, were harvested from *Bhmt*$^{+/+}$ (*black square*) and *Bhmt*$^{-/-}$ (*white square*) mice at various ages. *, $p < 0.01$, different from *Bhmt*$^{+/+}$ of the same age by Student's *t* test; $n = 10–16$ per group for 5–12-week-old mice and $n = 5$ per group for 20–48-week-old mice. *C,* morphology of GWAT and IWAT from 12-week-old mice was shown by hematoxylin-eosin staining. *Scale bar,* 50 μm. *D,* adipocyte cell area of GWAT and IWAT from 7- and 12-week-old *Bhmt*$^{+/+}$ (*black bar*) and *Bhmt*$^{-/-}$ (*white bar*) mice was analyzed using Zeiss AxioVision software. *, $p < 0.05$; **, $p < 0.01$, different from *Bhmt*$^{+/+}$ mice of the same age by Student's *t* test; $n = 3–5$ per group. *E,* BHMT protein in liver and adipose tissue from *Bhmt*$^{+/+}$ and *Bhmt*$^{-/-}$ mice were probed by Western blot analysis. The size of BHMT protein is 45 kDa. *F* and *G,* glucose tolerance test (*F*) and insulin tolerance test (*G*) were performed in 7-week-old *Bhmt*$^{+/+}$ (*black square*) and *Bhmt*$^{-/-}$ (*white square*) mice via intraperitoneal injection of either glucose or insulin and measuring tail blood glucose at various time points. *, $p < 0.05$, different from *Bhmt*$^{+/+}$ by Student's *t* test; $n = 7$ per group. Data are presented as mean ± S.E.

adipose tissue from both *Bhmt*$^{+/+}$ and *Bhmt*$^{-/-}$ mice (Fig. 1*E*), suggesting that the reduced fat mass in *Bhmt*$^{-/-}$ mice was due to an indirect effect of the lack of hepatic BHMT activity.

BHMT Deficiency Resulted in Enhanced Glucose Tolerance and Insulin Sensitivity—Changes in adiposity are often associated with alterations in glucose and insulin homeostasis. *Bhmt*$^{-/-}$ mice had normal basal blood glucose levels (Fig. 1, *F* and *G*). Upon intraperitoneal injection of either glucose (Fig. 1*F*) or insulin (Fig. 1*G*), *Bhmt*$^{-/-}$ mice exhibited a faster glucose removal rate than did wild type controls. *Bhmt*$^{-/-}$ mice also had a basal plasma insulin concentration that was 50% that of the controls ($p < 0.05$) (Table 2). These data indicated that *Bhmt*$^{-/-}$ mice had enhanced insulin sensitivity and glucose tolerance.

Bhmt$^{-/-}$ *Mice Had Increased Energy Expenditure*—To investigate the mechanisms that elicit the reduced fat mass in *Bhmt*$^{-/-}$ mice, elements of energy metabolism, including food intake, lipid uptake and absorption, body temperature, energy expenditure and activity, were determined. *Bhmt*$^{+/+}$ and *Bhmt*$^{-/-}$ mice consumed similar amounts of food per day (Fig. 2*A*). Fat load test (Fig. 2*B*) and fecal lipid content (Fig. 2*C*), tests for lipid uptake and absorption, respectively, displayed no differences between *Bhmt*$^{+/+}$ and *Bhmt*$^{-/-}$ mice. *Bhmt*$^{+/+}$ and *Bhmt*$^{-/-}$ mice had similar rectal temperatures (Fig. 2*D*). Compared with wild type controls, *Bhmt*$^{-/-}$ mice had increased O_2 consumption (Fig. 2*E* and Table 1) and increased CO_2 release (Fig. 2*F*) throughout the light and dark phases (Table 1), indicating increased energy expenditure. Locomotor activity was not increased in *Bhmt*$^{-/-}$ mice (Fig. 2*H*), suggesting that the increase in energy expenditure was independent of activity. The RER, an indicator of metabolic fuel preference, was not significantly different between *Bhmt*$^{+/+}$ and *Bhmt*$^{-/-}$ mice (Fig. 2*G*), although there was a trend of increasing RER during the light phase ($p = 0.053$) (Table 1).

Thermogenesis Was Not Increased in Bhmt$^{-/-}$ *Mice*—We next investigated whether the reduced adiposity observed in *Bhmt*$^{-/-}$ mice was due to increased thermogenesis. We predicted that *Bhmt*$^{-/-}$ mice would maintain a higher body temperature during a cold challenge if they had increased thermogenesis. After 6 h of cold exposure, the wild type controls dropped body temperature by 7.4% (from 38.18 ± 0.14 °C to 35.36 ± 0.07 °C), whereas *Bhmt*$^{-/-}$ mice dropped body temperature by 28.9% (from 37.92 ± 0.09 °C to 26.98 ± 2.15 °C) (Fig. 3*A*). Mice were removed from the cold room when body temperature was less than 28 °C. Brown adipose tissue (BAT) is a major site of nonshivering adaptive thermogenesis. We found no significant difference in the morphology or the weight of interscapular BAT between wild type and knock-out mice (data not shown). Real time PCR analysis revealed normal thermogenic gene responses in *Bhmt*$^{-/-}$ BAT tissue during cold exposure, with elevated *Pgc1* (peroxisome proliferator activated receptor γ coactivator), *Lpl* (lipoprotein lipase), *Ucp1* (uncoupling protein 1), and *Mcpt1* (muscle-type carnitine palmitoyltransferase 1) expression levels similar to those of *Bhmt*$^{+/+}$ mice (Fig. 3*B*), indicating that adrenergic signaling was intact and similar between genotypes. *Bhmt*$^{+/+}$ and *Bhmt*$^{-/-}$ mice had similar BAT TAG concentration before and after cold exposure, suggesting similar fuel storage and usage (Fig. 3*C*). Mice were also able to maintain body temperature using exogenous fuels derived from organs, such as white adipose tissue and liver via lipolysis and gluconeogenesis, and through adaptive thermogenesis involving shivering in skeletal muscle to increase energy output. Upon cold exposure, *Bhmt*$^{-/-}$ mice had significantly lower plasma glucose (by 46%, $p < 0.01$), glycerol (by 46%, $p < 0.05$), and NEFA (by 17%, $p < 0.05$) concentrations compared with those of wild type controls (Fig. 3, *D–F*), suggesting a restricted supply of exogenous fuels to maintain a normal body temperature. *Bhmt*$^{-/-}$ mice also had a significantly elevated plasma creatine kinase activity (by 1.76-fold, $p < 0.05$), a marker for muscle breakdown, perhaps because of increased shivering (Fig. 3*G*).

BHMT Deficiency Resulted in Altered Biochemical Measurements in Plasma—We examined whether genotypic differences in energy balance were accompanied by changes in plasma bio-

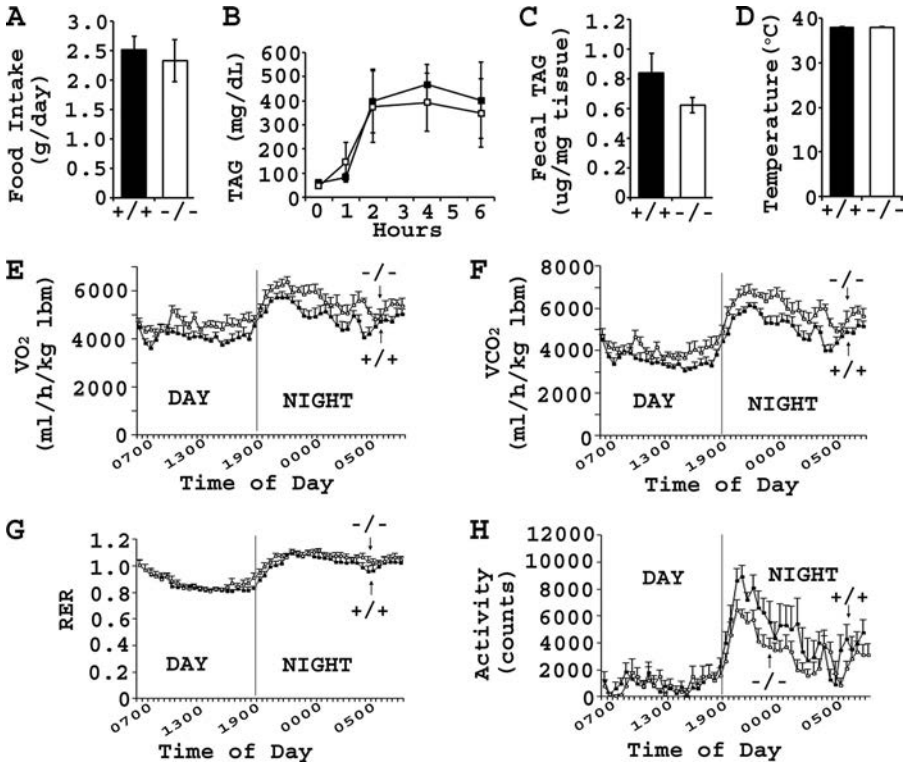

FIGURE 2. ***Bhmt*$^{-/-}$ mice had increased energy expenditure.** *A,* food intake was measured in 7-week-old *Bhmt*$^{+/+}$ (*black bar*) and *Bhmt*$^{-/-}$ (*white bar*) mice using an indirect calorimetry; $n = 8$ per group. *B,* fat tolerance test was performed in 7-week-old *Bhmt*$^{+/+}$ (*black square*) and *Bhmt*$^{-/-}$ (*white square*) mice via oral gavage of olive oil and measuring plasma TAG at various time points; $n = 3$ per group. *C,* fecal fat from *Bhmt*$^{+/+}$ (*black bar*) and *Bhmt*$^{-/-}$ (*white bar*) mice was extracted and measured using a colorimetric assay; $n = 7$ per group. *D,* rectal temperature of 7-week-old *Bhmt*$^{+/+}$ (*black bar*) and *Bhmt*$^{-/-}$ (*white bar*) mice was measured using a rectal probe thermometer at room temperature; $n = 6–7$ per group. *E–H,* oxygen consumption (*E*), carbon dioxide release (*F*), respiratory exchange ratio (CO_2 release/O_2 used) (*G*), and locomotor activity (*H*) were measured in 7-week-old *Bhmt*$^{+/+}$ (*black*) and *Bhmt*$^{-/-}$ (*white*) using an indirect calorimetry. Data were obtained after mice being acclimated to the chambers for 24 h and adjusted to lean body mass; $n = 8$ per group. Statistical analysis was as shown in Table 1. Data are presented as mean ± S.E. *VO_2,* oxygen consumption; *VCO_2,* carbon dioxide release.

TABLE 1

Indirect calorimetry data analysis

Oxygen consumption, carbon dioxide release, respiratory exchange ratio, and activity were measured in 7-week-old *Bhmt*$^{+/+}$ and *Bhmt*$^{-/-}$ mice using an indirect calorimetry; $n = 8$ per group. Data for light and dark cycles were obtained after mice were acclimated to the chambers for 24 h. VO_2 and VCO_2 were expressed based on either the body weight or the lean body mass (LBM). Area under the curve (AUC) on each measure was analyzed followed by *t* test and Mann-Whitney test. The unit of the AUC is *X* min, where *X* is the unit for each measure. Data are presented as mean ± S.E. VO_2, oxygen consumption; VCO_2, carbon dioxide release; MW test, Mann-Whitney test.

	Bhmt$^{+/+}$ AUC	*Bhmt*$^{-/-}$ AUC	*t*-test *p* value	MW test *p* value	Result
Light cycle					
VO_2 BW	2,336,800 ± 18,620	2,677,403 ± 78,771	0.003	0.0002	KO > WT
VO_2 LBM	2,914,726 ± 48,951	3,278,646 ± 99,639	0.006	0.007	KO > WT
VCO_2 BW	2,000,171 ± 24,476	2,358,855 ± 67,540	0.0008	0.0002	KO > WT
VCO_2 LBM	2,494,090 ± 38,538	2,888,922 ± 87,258	0.002	0.0003	KO > WT
RER	584 ± 6	600 ± 4	0.053	0.13	
Activity	1,007,037 ± 86,738	1,020,225 ± 173,692	0.95	0.69	
Dark cycle					
VO_2 BW	2,789,262 ± 52,593	3,207,252 ± 62,912	0.0002	0.0002	KO > WT
VO_2 LBM	3,477,415 ± 66,509	3,927,978 ± 86,540	0.001	0.0006	KO > WT
VCO_2 BW	2,880,493 ± 110,588	3,418,057 ± 69,089	0.001	0.002	KO > WT
VCO_2 LBM	3,582,632 ± 103,277	4,183,744 ± 83,270	0.0005	0.001	KO > WT
RER	720 ± 17	746 ± 10	0.21	0.16	
Activity	3,376,383 ± 421,560	2,351,641 ± 235,179	0.06	0.07	

chemical measurements. Basal plasma glycerol, NEFA, and glucose concentrations were similar for the two genotypes (Fig. 3, *D–F*). Basal plasma insulin concentration was 50% lower in *Bhmt*$^{-/-}$ mice than in controls ($p < 0.05$) (Table 2), suggesting a better insulin sensitivity. Plasma growth hormone and glucagon concentrations were not different between genotypes (Table 2). Because of the prominent role of thyroid hormone in controlling metabolic rate, we investigated whether increased thyroid hormone concentration contributed to the hypermetabolic phenotype in *Bhmt*$^{-/-}$ mice. Indeed, *Bhmt*$^{-/-}$ mice had a 33% increase in plasma T_4 (the major form of thyroid hormone in blood) concentration compared with that of wild type controls ($p < 0.05$) (Table 2). Plasma T_3 concentrations were not different between genotypes. Concentration of fibroblast growth factor 21 (FGF21), a recently discovered metabolic and glucose regulator, was found to be 1.75-fold higher in *Bhmt*$^{-/-}$ plasma than in *Bhmt*$^{+/+}$ plasma ($p < 0.01$) (Table 2). The increase in plasma FGF21 concentration observed in *Bhmt*$^{-/-}$

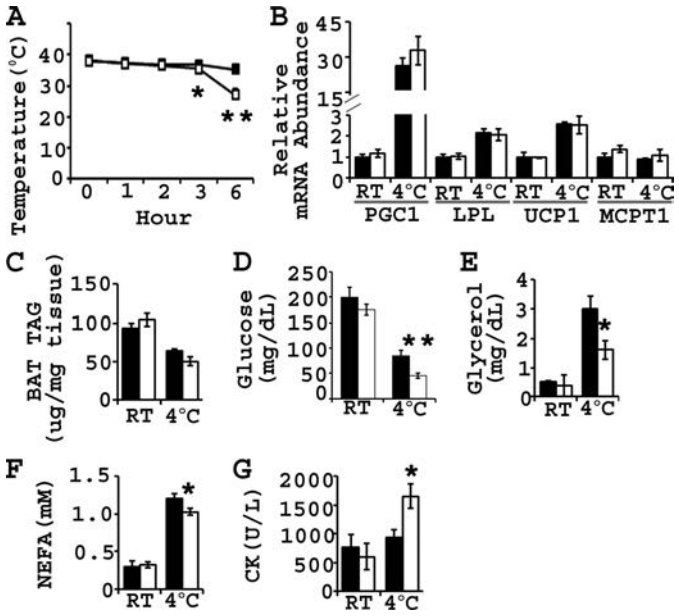

FIGURE 3. ***Bhmt*$^{-/-}$ mice were cold-sensitive due to lack of exogenous fuels.** Seven-week-old mice were exposed to room temperature or 4 °C, and tissues collected after 6 h of exposure. *A,* body temperature of *Bhmt*$^{+/+}$ (*black square*) and *Bhmt*$^{-/-}$ (*white square*) mice exposed to 4 °C was measured using a rectal probe thermometer at different time points. *, $p < 0.05$; **, $p < 0.01$, different from *Bhmt*$^{+/+}$ mice at the same time point by Student's *t* test; n = 13–14 per group. *B,* expression of genes involved in thermogenesis in the BAT of *Bhmt*$^{+/+}$ (*black bar*) and *Bhmt*$^{-/-}$ (*white bar*) mice at room temperature (n = 3–4 per group) or 4 °C (n = 7–8 per group) exposure. *C,* TAG in BAT from room temperature (n = 3–6 per group) or 4 °C (n = 13–14 per group) exposed *Bhmt*$^{+/+}$ (*black bar*) and *Bhmt*$^{-/-}$ (*white bar*) mice were extracted and measured colorimetrically. *D–G,* plasma glucose (*D*), glycerol (*E*), NEFA (*F*), and creatine kinase (*CK*) (*G*) from room temperature (n = 3–6 per group) or 4 °C (n = 13–14 per group) exposed *Bhmt*$^{+/+}$ (*black bar*) and *Bhmt*$^{-/-}$ (*white bar*) mice were measured colorimetrically. *, $p < 0.05$, different from *Bhmt*$^{+/+}$ mice under the same condition by Student's *t* test. Data are presented as mean ± S.E. *BAT,* brown adipose tissue; *NEFA,* nonesterified fatty acid; *CK,* creatine kinase; *PGC1α*, *pparγ* coactivator 1α; *LPL,* lipoprotein lipase; *UCP1,* uncoupling protein 1; *MCPT1,* muscle carnitine palmitoyl transferase 1.

TABLE 2

Metabolites and gene expression in *Bhmt*$^{+/+}$ and *Bhmt*$^{-/-}$ plasma and liver

Plasma and liver were collected from 7-week-old *Bhmt*$^{+/+}$ and *Bhmt*$^{-/-}$ mice after 4 h of fasting unless otherwise indicated. Plasma metabolites were measured using commercially available kits; n = 8–17 per group. Gene expression was measured by real time PCR, and expressed relatively to the controls; n = 6–10 per group. Glucose and glycogen were measured using an acid hydrolysis method; n = 6 per group.

Organ	Measurement	*Bhmt*$^{+/+}$	*Bhmt*$^{-/-}$
Plasma	Insulin (ng/ml) (7–12 weeks old)	0.806 ± 0.120	0.405 ± 0.157[a]
	FGF21 (ng/ml)	1.49 ± 0.16	2.6 ± 0.3[b]
	T_4 (μg/dl)	4.61 ± 0.27	5.73 ± 0.22[b]
	T_3 (ng/dl)	69.92 ± 5.87	75.37 ± 9.87
	Growth hormone (ng/ml)	5.02 ± 1.23	4.66 ± 1.46
	Glucagon (pg/ml)	39.68 ± 2.22	39.79 ± 1.08
Liver	FGF21 expression (relative abundance)	1.00 ± 0.24	3.35 ± 0.95[a]
	PPARα expression (relative abundance)	1.00 ± 0.20	1.16 ± 0.19
	PPARγ expression (relative abundance)	1.00 ± 0.51	3.57 ± 0.49[a]
	ChREBP expression (relative abundance)	1.00 ± 0.11	1.44 ± 0.15
	Glucose (μmol/g liver) (5 weeks old)	23.22 ± 0.91	18.22 ± 1.47[a]
	Glycogen (μmol/g liver) (5 weeks old)	100.13 ± 7.01	83.13 ± 4.21[a]

[a] $p < 0.05$.
[b] $p < 0.01$, different from *Bhmt*$^{+/+}$ by Students' *t* test. Data are presented as mean ± S.E.

mice was accompanied by a 3.35-fold increase in *Fgf21* expression in liver (where FGF21 is predominantly produced) compared with that of *Bhmt*$^{+/+}$ mice ($p < 0.05$). *Fgf21* expression is regulated by factors such as *Pparα* (peroxisome proliferator activated receptor-α), *Pparγ* (peroxisome proliferator activated receptor-γ), and *Chrebp* (carbohydrate response element) (16–19). Hepatic gene expression analysis revealed that *Bhmt*$^{-/-}$ mouse liver did not have altered expressions of *Pparα* and *Chrebp* but had increased expressions of *Pparγ* (by 3.5-fold, $p < 0.05$) as compared with the controls (Table 2).

BHMT Deficiency Resulted in Increased Bile Acids in Liver and Adipose Tissue—A novel concept indicating a signaling role of bile acids in the control of energy metabolism has emerged (20, 21). Increasing bile acid pool size in mice increased energy expenditure (21), while decreasing bile acid pool size reduced energy expenditure, resulting in weight gain and insulin resistance (20). Because *Bhmt*$^{-/-}$ mice had reduced plasma cholesterol (the precursor of bile acids) (2), we investigated whether *Bhmt* deletion altered the concentrations of bile acids. Cholic acid and chenodeoxycholic acid are the primary bile acids and are often conjugated with taurine (as taurocholate or taurochenodeoxycholate) or glycine (as glycocholate or glycochenodeoxycholate) forming bile salts. Compared with wild type littermates, *Bhmt* deletion resulted in 9.50- and 3.41-fold increases, respectively, in cholate ($p < 0.01$) and taurocholate ($p < 0.05$) in adipose tissue and in 2.33- and 1.62-fold increases, respectively, in taurocholate ($p < 0.05$) and glycocholate ($p < 0.01$) in liver (Table 3). Cholesterol is hydrolyzed to form 7-hydroxycholesterol, the precursor of bile acids. Compared with the controls, *Bhmt*$^{-/-}$ mice had reduced cholesterol (by 20%, $p < 0.05$) and increased 7-β-hydroxycholesterol (by 2.98-fold, $p < 0.05$) concentrations in the liver and increased 7-α-hydroxycholesterol (by 2.17-fold, $p < 0.01$) concentrations in the adipose tissue. These data suggest that *Bhmt* deletion enhanced the synthesis of bile acids from cholesterol and that the bile acids may contribute to the increased energy expenditure observed in *Bhmt*$^{-/-}$ mice.

Bhmt$^{-/-}$ *Mice Did Not Have Altered Lipolytic Rate*—To investigate whether the markedly decreased adiposity observed in *Bhmt*$^{-/-}$ mice was due to increased lipolysis, we measured lipolytic rates in both *in vivo* and *ex vivo* models where lipolytic stimuli were given, and glycerol released was measured as the indicator of lipolytic rate. Plasma TAG and glucose were also measured in the *in vivo* model to determine the whole body response to adrenergic stimuli. During the *in vivo* experiment, when CL316243 (β_3-adrenergic specific lipolytic stimulus) was administered, *Bhmt*$^{+/+}$ and *Bhmt*$^{-/-}$ mice had similar levels of plasma TAG, glycerol, and glucose release (Fig. 4, *A–C*). When isoproterenol (nonspecific lipolytic stimulus) was administered, *Bhmt*$^{+/+}$ and *Bhmt*$^{-/-}$ mice had similar levels of plasma TAG and glycerol (Fig. 4, *A* and *B*) but had a 50% decreased plasma glucose concentration compared with wild type controls ($p < 0.05$) (Fig. 4*C*), indicating a deficiency in hepatic glucose storage or generation. Measurements of hepatic glucose and glycogen concentrations revealed that *Bhmt*$^{-/-}$ mice had reduced hepatic glucose (by 22%, $p < 0.05$) and glycogen (by 17%, $p < 0.05$) concentrations compared with those of *Bhmt*$^{+/+}$ mice (Table 2). These data perhaps explain why *Bhmt*$^{-/-}$ mice had lower plasma glucose concentration during cold exposure and nonspecific lipolysis tests. Lipolysis was further analyzed in isolated GWAT and IWAT explants from *Bhmt*$^{+/+}$ and *Bhmt*$^{-/-}$ mice. The explants from *Bhmt*$^{-/-}$ mice released similar amounts of glycerol as did those from *Bhmt*$^{+/+}$

TABLE 3

Bile acids and sterols in $Bhmt^{+/+}$ and $Bhmt^{-/-}$ liver and adipose tissue

Liver and gonadal adipose tissue were collected from 5-week-old $Bhmt^{+/+}$ and $Bhmt^{-/-}$ mice after 4 h of fasting; $n = 6$ per group. The amount and the relative abundance of metabolites were measured and analyzed by liquid and gas chromatography by mass spectrometry. Data are presented as mean ± S.E.

Metabolites	$Bhmt^{+/+}$ mean counts	$Bhmt^{-/-}$ mean counts	-Fold change	*p* value	Result
Liver					
Cholate	0.84 ± 0.08	2.26 ± 0.78	2.71	0.184	
Taurocholate	0.75 ± 0.09	1.21 ± 0.12	1.62	0.010	KO > WT
Glycocholate	0.88 ± 0.18	1.95 ± 0.43	2.33	0.021	KO > WT
Taurochenodeoxycholate	1.62 ± 0.44	0.88 ± 0.22	0.54	0.228	
Cholesterol	1.19 ± 0.07	0.95 ± 0.06	0.80	0.036	WT > KO
7-β-Hydroxycholesterol	0.76 ± 0.45	2.26 ± 0.71	2.98	0.020	KO > WT
Adipose					
Cholate	0.94 ± 0.23	8.93 ± 2.88	9.50	0.005	KO > WT
Taurocholate	1.14 ± 0.31	3.90 ± 0.96	3.41	0.020	KO > WT
Cholesterol	1.09 ± 0.08	1.25 ± 0.10	1.15	0.261	
7-α-hydroxycholesterol	0.88 ± 0.19	1.92 ± 0.20	2.17	0.009	KO > WT
7-β-hydroxycholesterol	1.03 ± 0.18	1.53 ± 0.21	1.48	0.075	

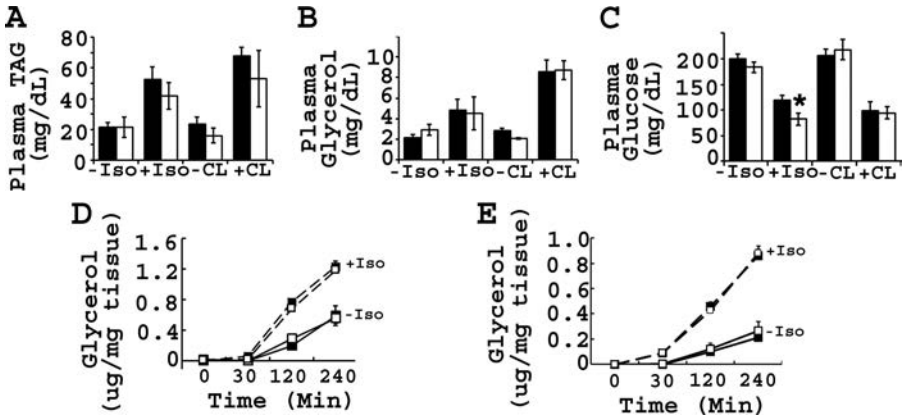

FIGURE 4. ***Bhmt*$^{-/-}$ mice had normal lipolytic responses.** *A–C,* plasma TAG (*A*), glycerol (*B*), and glucose (*C*) were measured in 7-week-old $Bhmt^{+/+}$ (*black bar*) and $Bhmt^{-/-}$ (*white bar*) mice before and after i.p. injection of lipolytic stimulus isoproterenol or CL316243; $n = 5–7$ per group. *D* and *E,* gonadal (*D*) or inguinal (*E*) explants from $Bhmt^{+/+}$ (*black square*) and $Bhmt^{-/-}$ (*white square*) mice were used to measure glycerol release without (*solid line*) or with (*dashed line*) 10 μM lipolytic stimulus isoproterenol; $n = 4–6$ per group. Data are presented as mean ± S.E. *Iso,* isoproterenol; *CL,* CL CL316243.

mice under basal or stimulated conditions (Fig. 4, *D* and *E*), suggesting normal lipolytic machinery in $Bhmt^{-/-}$ mice.

BHMT Deficiency Resulted in Impaired TAG Synthesis and Enhanced Glucose Oxidation in Isolated Mature Adipocytes and Impaired TAG Oxidation in Liver Homogenates—Because TAG breakdown was not defective, we assessed whether TAG synthesis and FA oxidation were altered within the fat cells. We isolated mature adipocytes from both GWAT and IWAT from $Bhmt^{-/-}$ mice and their littermate controls and measured the rates of [1-^{14}C]oleate incorporation into TAG (for TAG synthesis), into CO_2 (for complete FA oxidation) and acid-soluble metabolites (for incomplete FA oxidation). Mature adipocytes isolated from $Bhmt^{+/+}$ and $Bhmt^{-/-}$ GWAT had the same rate of TAG synthesis (Fig. 5*A*). Interestingly, mature adipocytes isolated from $Bhmt^{-/-}$ IWAT made less TAG (by 62%) compared with that of $Bhmt^{+/+}$ mice ($p < 0.001$). GWAT and IWAT adipocytes from $Bhmt^{+/+}$ and $Bhmt^{-/-}$ mice had the same FA oxidation rate (Fig. 5*B*), indicating normal β-oxidation machinery. Because several lines of evidence (enhanced glucose tolerance and insulin sensitivity, reduced glucose upon cold exposure and isoproterenol stimulus, and reduced hepatic glucose storage) suggested an increased reliance on glucose in $Bhmt^{-/-}$ mice, we assessed whether their mature adipocytes used more glucose. At basal level (without insulin), mature adipocytes isolated from $Bhmt^{+/+}$ and $Bhmt^{-/-}$ GWAT had the same glucose oxidation rate (Fig. 5*C*). However, with insulin treatment, $Bhmt^{-/-}$ GWAT oxidized 2.38-fold more glucose than did $Bhmt^{+/+}$ GWAT ($p < 0.05$). Mature adipocytes isolated from $Bhmt^{-/-}$ IWAT oxidized 2.4- and 1.78-fold more glucose than did $Bhmt^{+/+}$ IWAT without and with insulin treatment ($p < 0.01$) (Fig. 5*D*). Compared with the basal level, insulin treatment induced glucose oxidation by 1.87-, 4.17-, 3.21-, and 3.79-fold, respectively, for $Bhmt^{+/+}$ GWAT, $Bhmt^{-/-}$ GWAT, $Bhmt^{+/+}$ IWAT, and $Bhmt^{-/-}$ IWAT, confirming the viability of the isolated mature adipocytes, and indicating a higher response to insulin in $Bhmt^{-/-}$ mice, particularly in GWAT (Fig. 5, *C* and *D*). Because $Bhmt^{-/-}$ mice had fatty liver (2), we also investigated the possibility that *Bhmt* deficiency might lead to impaired hepatic fatty acid oxidation. FA oxidation rate was determined using liver homogenates from $Bhmt^{+/+}$ and $Bhmt^{-/-}$ mice. $Bhmt^{-/-}$ mouse liver released 60% less CO_2 than did $Bhmt^{+/+}$ mouse liver, suggesting impaired complete FA oxidation ($p < 0.03$) (Fig. 5, *E* and *F*).

Betaine Supplementation Increased Hepatic Fgf21 Expression—Betaine is commonly used in the livestock and poultry industries to generate leaner meats (22), and FGF21 is a novel metabolic regulator (23). *Bhmt* ablation resulted in a significant accumulation of betaine in many tissues (2), and in increased hepatic *Fgf21* expression as well as circulating FGF21 protein (Table 2). To investigate the potential interaction between

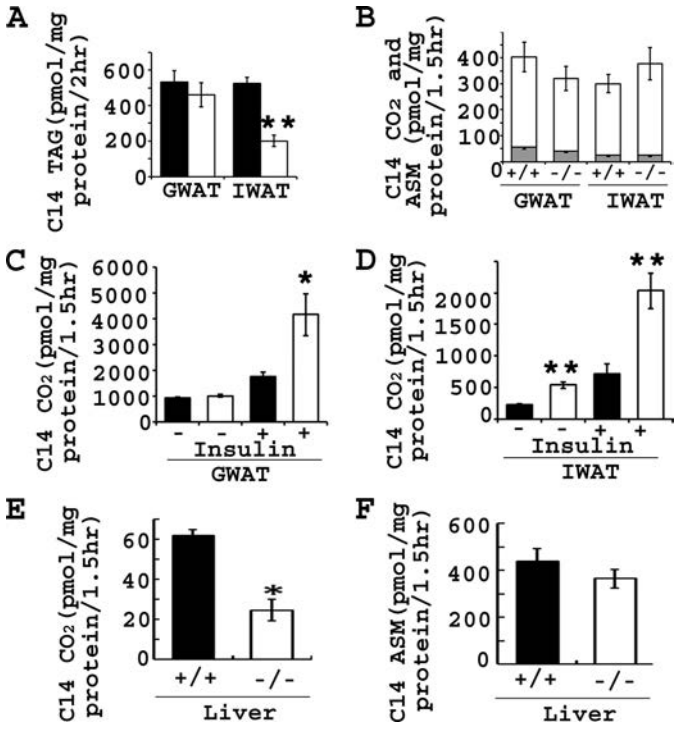

FIGURE 5. ***Bhmt*$^{-/-}$ mouse adipocytes had altered TAG synthesis and glucose oxidation.** *A,* mature adipocytes were isolated from *Bhmt*$^{+/+}$ (*black bar*) and *Bhmt*$^{-/-}$ (*white bar*) mice GWAT and IWAT and used to determine the rate of labeled fatty acid incorporated to triacylglycerol. **, $p < 0.01$, different from *Bhmt*$^{+/+}$ mice by Student's *t* test; $n = 4–5$ per group. *B,* mature adipocytes were isolated from *Bhmt*$^{+/+}$ and *Bhmt*$^{-/-}$ mice GWAT and IWAT and used to determine the rate of ^{14}C 18:1 oxidation: CO_2 (*gray bar*), ASM (*white bar*); $n = 10–13$ per group. *C* and *D,* mature adipocytes were isolated from *Bhmt*$^{+/+}$ (*black bar*) and *Bhmt*$^{-/-}$ (*white bar*) mice GWAT (*C*) and IWAT (*D*) and used to determine the rate of glucose oxidation with or without insulin. *, $p < 0.05$; **, $p < 0.01$ different from *Bhmt*$^{+/+}$ mice under the same treatment by Student's *t* test; $n = 7–10$ per group without insulin, $n = 4–7$ per group with insulin. *E* and *F,* liver homogenates from *Bhmt*$^{+/+}$ (*black bar*) and *Bhmt*$^{-/-}$ (*white bar*) mice were used to determine the rate of ^{14}C 18:1 oxidation. *, $p < 0.05$, different from *Bhmt*$^{+/+}$ mice by Student's *t* test $n = 5–7$ per group Data are presented as mean ± S.E.

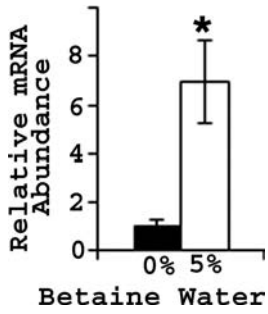

FIGURE 6. **Betaine supplementation increased hepatic *Fgf21* expression.** 7-Week-old *Bhmt*$^{+/+}$ mice were fed either a 0 or a 5% betaine supplemented water for 2 weeks. Livers were collected for the measurement of *Fgf21* expression using real time PCR. Expression was expressed relatively to the controls; $n = 6–8$ per group. *, $p < 0.05$, different from 0% group by Student's *t* test. Data are presented as mean ± S.E.

betaine and FGF21, wild type mice were fed either 0 or 5% betaine supplemented water for 2 weeks. A 5% betaine supplemented water was selected based on our experience, that this concentration did not alter food or water intake in mice (data not shown). Interestingly, at 2 weeks, 5% betaine water feeding increased *Fgf21* expression by almost 7-fold in wild type liver ($p < 0.05$) (Fig. 6).

DISCUSSION

BHMT is one of the most abundant proteins in the liver, representing 0.6–1.6% of the total protein (24). However, its known functions are limited to its roles in choline and one-carbon metabolism. Our current studies establish a unique role for BHMT in energy homeostasis.

Previously, we found that *Bhmt*$^{-/-}$ mice had reduced body weight from 5 to 9 weeks of age compared with wild type littermates, although the difference in body weight disappeared after 9 weeks (2). MRI and dissection of fat pads revealed that the reduced body weight in *Bhmt*$^{-/-}$ mice was due to lower fat mass. *Bhmt*$^{-/-}$ mice had smaller fat pad mass that persisted through at least 1 year of age compared with the controls. *Bhmt*$^{-/-}$ mice were able to maintain body weight in light of the reduced fat mass after 9 weeks of age perhaps because they had heavier livers that made up for the difference in fat mass weight (2). For example, at 12 weeks of age, *Bhmt*$^{-/-}$ mice had an average liver weight 409 mg heavier than that of *Bhmt*$^{+/+}$ mice (1.85 ± 0.08 g in *Bhmt*$^{-/-}$ mice *versus* 1.44 ± 0.06 g in *Bhmt*$^{+/+}$ mice), which made up for the difference in fat pad mass (511 ± 39 mg in *Bhmt*$^{-/-}$ mice *versus* 815 ± 74 mg in *Bhmt*$^{+/+}$ mice). BHMT is a liver-specific enzyme in rodents (1). Because BHMT protein was absent in normal adipose tissue, this observation indicated that the reduced fat mass in *Bhmt*$^{-/-}$ mice was due to an indirect effect of the lack of hepatic BHMT activity. How could lack of an hepatic enzyme result in reduced fat mass? One possibility is diminished lipid transport from the liver to adipose tissue via very low density lipoprotein (VLDL). Our previous work showed that *Bhmt*$^{-/-}$ mice had reduced hepatic PtdCho concentration, resulting in decreased VLDL secretion and increased hepatic fat accumulation (2). However, the amount of fat missing in fat pads exceeds the excess amount of fat accumulated in the liver. In addition, adipose should be able to store lipid obtained from the diet instead of depending solely on hepatic lipid sources. Thus, decreased VLDL secretion is unlikely to account for all the fat absence. Homeostasis of energy stores is regulated by mechanisms that include modulation of metabolic rate and thermogenesis, control of metabolite fluxes among various organs, and modulation of fuel synthesis and usage within adipose tissue. Examination of each of these parameters in *Bhmt*$^{-/-}$ mice showed that multiple factors might contribute to the reduced adiposity observed in this mouse model.

Compared with the controls, *Bhmt*$^{-/-}$ mice had better glucose tolerance and insulin sensitivity. Glucose concentrations measured after a 4-h fast were about 200 mg/dl for both *Bhmt*$^{+/+}$ and *Bhmt*$^{-/-}$ mice. Glucose concentrations measured after a 16-h fast were higher in *Bhmt*$^{+/+}$ (158 ± 6 mg/dl) than in *Bhmt*$^{-/-}$ mice (119 ± 10 mg/dl, $p < 0.05$). Glucose values were at the high end of what have been reported for C57Bl mice (130–218 mg/dl for a 4-h fast (25–29) and 90–120 mg/dl for a 12–16 h fast (27, 30)).

Bhmt$^{-/-}$ mice had normal food intake, fat clearance rate, and fecal fat content, indicating that the reduced adiposity was not due to reduced energy intake or fat malabsorption. *Bhmt*$^{-/-}$ mice had increased rates of O_2 consumption and CO_2

release, suggesting that the reduced fat mass was partially due to increased energy utilization. Because locomotor activity did not differ between genotypes, the increased energy expenditure exhibited by *Bhmt*$^{-/-}$ mice was not due to increased physical activity. We investigated whether the reduced adiposity was due to increased thermogenesis. Upon cold exposure, *Bhmt*$^{-/-}$ mice failed to maintain their body temperature. *Bhmt*$^{-/-}$ mice exhibited normal induction of genes involved in mitochondrial biogenesis, uncoupling, and fatty acid oxidation in BAT. Furthermore, *Bhmt*$^{-/-}$ mice had normal BAT TAG storage and functional lipolytic machinery in peripheral tissues. However, during prolonged cold exposure, *Bhmt*$^{-/-}$ mice had lower plasma glucose, glycerol, and NEFA and higher plasma creatine kinase (marker of muscle breakdown). These data indicated that *Bhmt*$^{-/-}$ mice were not hyperthermogenic. In fact, these animals were cold-sensitive due to lack of exogenous fuel and had to depend on shivering thermogenesis in an attempt to maintain body temperature. The reduced plasma glucose concentration in *Bhmt*$^{-/-}$ mice during cold exposure was probably because they had less hepatic glucose stored. The reduced plasma glycerol and NEFA concentrations in *Bhmt*$^{-/-}$ mice during cold exposure were probably because they had less TAG stored in the adipose tissue to be released during energy needs. It was also possible that the *Bhmt*$^{-/-}$ mouse liver was taking up glycerol more efficiently than did *Bhmt*$^{+/+}$ for glucose synthesis to make up for the lack of hepatic glucose.

Within the adipose tissue, we observed that *Bhmt*$^{-/-}$ IWAT, but not GWAT, made 62% less TAG than did the controls. Although *Bhmt*$^{-/-}$ mice had normal lipolytic and FA oxidation machinery in both fat depots, the mice might have less TAG stored at a time when fuel was needed. We suspected that *Bhmt*$^{-/-}$ mice might utilize more glucose instead of FA as fuel. Indeed, we observed increased glucose oxidation in *Bhmt*$^{-/-}$ GWAT with insulin stimulus, and increased glucose oxidation in *Bhmt*$^{-/-}$ IWAT with or without insulin stimulus. This hypothesis was further supported by the enhanced glucose tolerance and insulin sensitivity observed in *Bhmt*$^{-/-}$ mice, the reduced plasma glucose during cold exposure, β-adrenergic stimulation, 16 h of fasting, and the reduced hepatic glucose storage. Enhanced glucose oxidation in adipose tissue and reduced hepatic glucose storage could potentially limit the availability of acetyl-CoA for forming fatty acids and the availability of the glycerol backbone for forming TAG, contributing to reduced adiposity. These data also suggested that the altered fuel metabolism in *Bhmt*$^{-/-}$ mice was not limited to adipose tissue but also occurred in the liver. *Bhmt*$^{-/-}$ mice had fatty liver and lower hepatic glucose concentrations, suggesting the possibility of FA utilization impairment. Indeed, we found *Bhmt*$^{-/-}$ mouse liver burned less FA as compared with *Bhmt*$^{+/+}$ mouse liver.

It is intriguing that the observed effects were more pronounced in IWAT as compared with GWAT in *Bhmt*$^{-/-}$ mice. The size of 12-week-old *Bhmt*$^{-/-}$ GWAT adipocytes was 57% that of controls, although IWAT adipocytes size was 20% the size of that in controls. Adipocytes from *Bhmt*$^{-/-}$ IWAT synthesized 62% less TAG and oxidized 2.4-fold more glucose than did control IWAT, although no changes were detected in adipocytes from GWAT. It is commonly accepted that visceral (GWAT) and subcutaneous (IWAT) fat pads are different. GWAT is considered to be the "pure WAT," whereas IWAT is a "convertible WAT" that may convert to BAT (31). Compared with visceral fat, subcutaneous fat cells express more thyroid hormone receptors (32) and mitochondrial *Ucp1* (33, 34), have more efficient insulin signaling and *Glut4* (35), and are more responsive to *Ppar*γ thiazolidinedione ligand (36, 37). When subcutaneous fat was transplanted into the visceral cavity of mice, it reduced body weight and fat mass and enhanced insulin and glucose sensitivities (38), suggesting an intrinsic difference between the two fat pads. These differences in GWAT and IWAT may explain why effects in *Bhmt*$^{-/-}$ IWAT are more pronounced. Other investigators also report metabolic differences between GWAT and IWAT (39).

Bhmt$^{-/-}$ mice had reduced adiposity due to increased energy expenditure, enhanced glucose oxidation in WAT, and reduced TAG synthesis in WAT. The next question was how *Bhmt* deficiency could exert these differences, and we identified several candidate mechanisms that may be responsible. Coinciding with increased energy expenditure, *Bhmt*$^{-/-}$ mice had elevated plasma T_4 (the major form of thyroid hormone in the blood), a well known energy metabolism regulator. Plasma T_4 is converted to T_3, the active form of thyroid hormone, with tissues. Unfortunately, we were unable to measure the conversion of T_4 to T_3 and T_3 concentration within tissues. Another potential candidate that may be responsible for these metabolic changes in *Bhmt*$^{-/-}$ mice is FGF21. *Bhmt*$^{-/-}$ mice overexpressed hepatic *Fgf21* and had elevated plasma FGF21 concentration. FGF21 is a novel metabolic regulator that is preferentially expressed in the liver (23). FGF21 increases glucose uptake (40, 41) and decreases intracellular TAG content in adipocytes (40); it lowers plasma glucose and TAG when administered to diabetic mice (41); and it increases energy expenditure and improves insulin sensitivity in diet-induced obese mice (42, 43). Another potential candidate is bile acid. Recent studies suggested a role of bile acids in glucose and energy homeostasis. Mice fed a cholic acid (a bile acid)-supplemented diet had increased energy expenditure, preventing obesity and insulin resistance (21), although mice with reduced bile acids had decreased energy expenditure (20). *Bhmt* deletion resulted in increased cholate and taurocholate in adipose tissue and in increased taurocholate and glycocholate in liver. *Bhmt*$^{-/-}$ mice had reduced hepatic and serum cholesterol (2). This was perhaps due to an increased conversion of cholesterol to cholic acid. Indeed, the concentration of 7-hydroxycholesterol, the precursor to bile acid from cholesterol, was significantly elevated in both liver and adipose in *Bhmt*$^{-/-}$ mice.

Thyroid hormone, FGF21, and bile acids all induce similar metabolic changes and were all altered in *Bhmt*$^{-/-}$ mice. In fact, a growing body of evidence suggests an interaction among bile acids, thyroid hormone, and FGF21. Thyroid hormone induced cholesterol 7α-hydroxylase (CYP7A1), the rate-limiting enzyme in bile acid synthesis from cholesterol (44, 45), and there was an inverse relationship between thyroid hormone level and serum cholesterol (46). Thyroid hormone also induced hepatic *Fgf21* expression in mice (47). Bile acids enhanced the conversion of T_4 to T_3 within tissues, resulting in

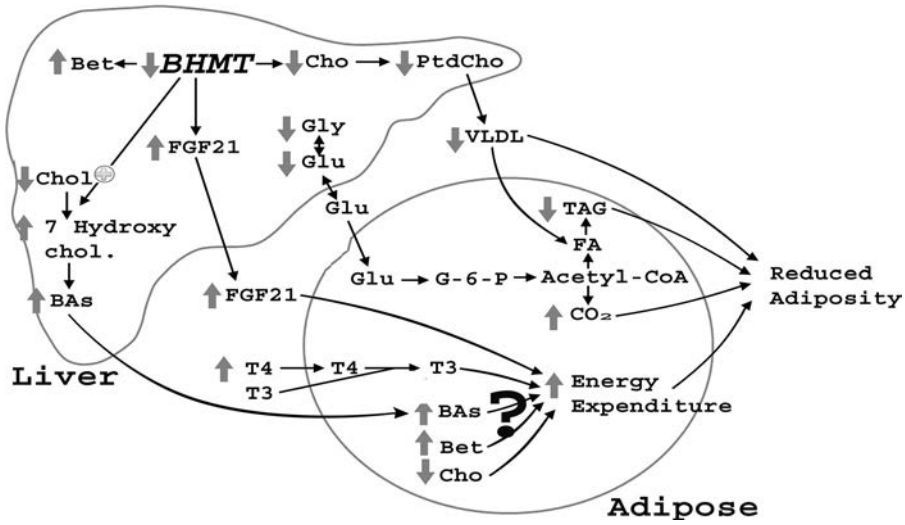

FIGURE 7. **Overview of metabolic disturbances in *Bhmt*$^{-/-}$ mice.** Increased energy expenditure, decreased lipid mobilization from the liver to adipose tissue, decreased TAG synthesis, and enhanced glucose oxidation together resulted in reduced fat mass in *Bhmt*$^{-/-}$ mice. *Bhmt* deletion increased plasma FGF21 and T_4 concentrations and increased betaine and bile acids concentrations while decreased choline concentration in both liver and adipose tissue. All of these changes had been associated with increased energy expenditure, enhanced insulin sensitivity, and reduced adiposity, and might be interrelated with one another. *BHMT,* betaine-homocysteine *S*-methyltransferase; *Cho,* choline; *Bet,* betaine; *FGF21,* fibroblast growth factor 21; *Chol,* cholesterol; *7 hydroxychol,* 7-hydroxycholesterol; *BAs,* bile acids; *Glu,* glucose; *Gly*, glycogen; *G-6-P,* glucose 6-phosphate.

increased energy expenditure in mice (21). Both bile acids and FGF21 concentrations were elevated in patients with nonalcoholic fatty liver (48). These studies suggest an interaction among these factors and *Bhmt* deficiency, resulting in reduced adiposity observed in *Bhmt*$^{-/-}$ mice.

Aside from the increased bile acids, thyroid hormone, and FGF21, deletion of hepatic *Bhmt* may cause reduced adiposity via changes in choline metabolites. As mentioned previously, BHMT is a major regulator of choline metabolism. Deletion of *Bhmt* resulted in altered choline metabolites, including a 21- and 2-fold increase in hepatic and adipose tissue betaine concentrations and an 82 and 53% decrease in hepatic and adipose tissue choline concentrations (2). Recently, studies suggested that manipulation of dietary choline or alteration of pathways in choline metabolism may influence energy expenditure and adiposity. Mice fed a methionine- and choline-deficient diet were hypermetabolic, lost weight (49), and had better insulin sensitivity and glucose tolerance (50). Mice with the *Pemt* gene (making PtdCho from phosphatidylethanolamine) deleted had normal metabolic parameters on a regular chow diet compared with wild type controls; however, when fed a high fat diet, they had increased oxygen consumption and RER, accumulated less body fat, and had increased glucose sensitivity (51). The lack of weight gain in *Pemt*$^{-/-}$ mice disappeared when mice were supplemented with choline. These observations suggest a potential role of choline in modulating energy metabolism. Similar to methionine- and choline-deficient diet fed mice and the *Pemt*$^{-/-}$ mice, *Bhmt*$^{-/-}$ mice had reduced choline and PtdCho concentrations, enhanced glucose and insulin sensitivities, increased energy expenditure, and reduced adiposity.

Bhmt ablation also resulted in a significant accumulation of betaine, which serves as a methyl donor and osmolyte. Betaine is commercially available as a feed additive; it is widely discussed as a "carcass modifier" because of its lipotropic and growth-promoting effects, generating leaner meat (22). Dietary betaine supplementation resulted in reduced abdominal fat in poultry and reduced carcass fat (by 10–18%) in pigs (22). The exact mechanism by which betaine modulates carcass quality is still unclear but has been suggested to involve interactions of betaine with growth factors and thyroid hormones (52–60). We did not observe increased growth hormone but did observe enhanced plasma T_4 and FGF21 concentrations and consequently hypermetabolism in *Bhmt*$^{-/-}$ mice. Betaine may also have a role as a glucose sensitizer. Betaine supplementation enhanced insulin sensitivity in diet-induced obese mice and increased insulin signaling pathway in isolated adipocytes (61). We found that 2 weeks of 5% betaine feeding increased *Fgf21* expression by 7-fold in wild type liver. How betaine increases *Fgf21* expression and whether FGF21 is responsible for the reduced adiposity phenotype in *Bhmt*$^{-/-}$ mice warrant more studies.

To summarize (Fig. 7), *Bhmt* deletion resulted in reduced adiposity, enhanced insulin sensitivity, and glucose tolerance. The reduction in fat mass in *Bhmt*-deficient mice could be attributed to increased whole body energy expenditure, decreased mobilization of lipids from the liver (VLDL) to be stored in adipose tissues, decreased TAG synthesis in white adipose tissue, and increased glucose oxidation in white adipose tissue. Deletion of *Bhmt* resulted in a variety of biochemical abnormalities, including elevated thyroid hormone, bile salts, FGF21 and betaine concentrations, and reduced choline and PtdCho concentrations. Many of these changes have been related to elevated energy metabolism, reduced adiposity, and enhanced glucose tolerance and insulin sensitivity. How these parameters interact with each other warrants further studies. This study suggests a role of *Bhmt* in regulating energy metabolism and adiposity.

REFERENCES

1. Szegedi, S. S., Castro, C. C., Koutmos, M., and Garrow, T. A. (2008) Betaine-homocysteine *S*-methyltransferase-2 is an *S*-methylmethionine-homocysteine methyltransferase. *J. Biol. Chem.* **283,** 8939–8945
2. Teng, Y. W., Mehedint, M. G., Garrow, T. A., and Zeisel, S. H. (2011) Deletion of betaine-homocysteine *S*-methyltransferase in mice perturbs choline and 1-carbon metabolism, resulting in fatty liver and hepatocellular carcinomas. *J. Biol. Chem.* **286,** 36258–36267
3. Ji, C., Shinohara, M., Vance, D., Than, T. A., Ookhtens, M., Chan, C., and Kaplowitz, N. (2008) Effect of transgenic extrahepatic expression of betaine-homocysteine methyltransferase on alcohol or homocysteine-induced fatty liver. *Alcohol. Clin Exp. Res.* **32,** 1049–1058
4. Delgado-Reyes, C. V., Wallig, M. A., and Garrow, T. A. (2001) Immunohistochemical detection of betaine-homocysteine *S*-methyltransferase in human, pig, and rat liver and kidney. *Arch. Biochem. Biophys.* **393,** 184–186
5. Folch, J., Lees, M., and Sloane Stanley, G. H. (1957) A simple method for the isolation and purification of total lipids from animal tissues. *J. Biol. Chem.* **226,** 497–509
6. Passonneau, J. V., and Lauderdale, V. R. (1974) A comparison of three methods of glycogen measurement in tissues. *Anal. Biochem.* **60,** 405–412
7. Boudonck, K. J., Mitchell, M. W., Német, L., Keresztes, L., Nyska, A., Shinar, D., and Rosenstock, M. (2009) Discovery of metabolomics biomarkers for early detection of nephrotoxicity. *Toxicol. Pathol.* **37,** 280–292
8. Evans, A. M., DeHaven, C. D., Barrett, T., Mitchell, M., and Milgram, E. (2009) Integrated, nontargeted ultrahigh performance liquid chromatography/electrospray ionization tandem mass spectrometry platform for the identification and relative quantification of the small molecule complement of biological systems. *Anal. Chem.* **81,** 6656–6667
9. Lawton, K. A., Berger, A., Mitchell, M., Milgram, K. E., Evans, A. M., Guo, L., Hanson, R. W., Kalhan, S. C., Ryals, J. A., and Milburn, M. V. (2008) Analysis of the adult human plasma metabolome. *Pharmacogenomics* **9,** 383–397
10. Barrett, T., Dehaven, C. D., and Alexander, D. C. (October 27, 2008) U. S. Patent 7,433,787
11. Jaworski, K., Ahmadian, M., Duncan, R. E., Sarkadi-Nagy, E., Varady, K. A., Hellerstein, M. K., Lee, H. Y., Samuel, V. T., Shulman, G. I., Kim, K. H., de Val, S., Kang, C., and Sul, H. S. (2009) AdPLA ablation increases lipolysis and prevents obesity induced by high fat feeding or leptin deficiency. *Nat. Med.* **15,** 159–168
12. Warne, J. P., John, C. D., Christian, H. C., Morris, J. F., Flower, R. J., Sugden, D., Solito, E., Gillies, G. E., and Buckingham, J. C. (2006) Gene deletion reveals roles for annexin A1 in the regulation of lipolysis and IL-6 release in epididymal adipose tissue. *Am. J. Physiol. Endocrinol. Metab.* **291,** E1264–E1273
13. Viswanadha, S., and Londos, C. (2006) Optimized conditions for measuring lipolysis in murine primary adipocytes. *J. Lipid Res.* **47,** 1859–1864
14. Bligh, E. G., and Dyer, W. J. (1959) A rapid method of total lipid extraction and purification. *Can. J. Biochem. Physiol.* **37,** 911–917
15. Lillie, R. (1965) *Histopathologic Technic and Practical Histochemistry,* 3rd Ed., pp. 1–715, McGraw-Hill Book Co., New York
16. Moyers, J. S., Shiyanova, T. L., Mehrbod, F., Dunbar, J. D., Noblitt, T. W., Otto, K. A., Reifel-Miller, A., and Kharitonenkov, A. (2007) Molecular determinants of FGF-21 activity-synergy and cross-talk with PPARγ signaling. *J. Cell. Physiol.* **210,** 1–6
17. Oishi, K., and Tomita, T. (2011) Thiazolidinediones are potent inducers of fibroblast growth factor 21 expression in the liver. *Biol. Pharm. Bull.* **34,** 1120–1121
18. Iizuka, K., Takeda, J., and Horikawa, Y. (2009) Glucose induces FGF21 mRNA expression through ChREBP activation in rat hepatocytes. *FEBS Lett.* **583,** 2882–2886
19. Sánchez, J., Palou, A., and Picó, C. (2009) Response to carbohydrate and fat refeeding in the expression of genes involved in nutrient partitioning and metabolism: striking effects on fibroblast growth factor-21 induction. *Endocrinology* **150,** 5341–5350
20. Watanabe, M., Horai, Y., Houten, S. M., Morimoto, K., Sugizaki, T., Arita, E., Mataki, C., Sato, H., Tanigawara, Y., Schoonjans, K., Itoh, H., and Auwerx, J. (2011) Lowering bile acid pool size with a synthetic farnesoid X receptor (FXR) agonist induces obesity and diabetes through reduced energy expenditure. *J. Biol. Chem.* **286,** 26913–26920
21. Watanabe, M., Houten, S. M., Mataki, C., Christoffolete, M. A., Kim, B. W., Sato, H., Messaddeq, N., Harney, J. W., Ezaki, O., Kodama, T., Schoonjans, K., Bianco, A. C., and Auwerx, J. (2006) Bile acids induce energy expenditure by promoting intracellular thyroid hormone activation. *Nature* **439,** 484–489
22. Eklund, M., Bauer, E., Wamatu, J., and Mosenthin, R. (2005) Potential nutritional and physiological functions of betaine in livestock. *Nutr. Res. Rev.* **18,** 31–48
23. Nishimura, T., Nakatake, Y., Konishi, M., and Itoh, N. (2000) Identification of a novel FGF, FGF-21, preferentially expressed in the liver. *Biochim. Biophys. Acta* **1492,** 203–206
24. Pajares, M. A., and Pérez-Sala, D. (2006) Betaine-homocysteine *S*-methyltransferase. Just a regulator of homocysteine metabolism? *Cell. Mol. Life Sci.* **63,** 2792–2803
25. Rajala, M. W., Qi, Y., Patel, H. R., Takahashi, N., Banerjee, R., Pajvani, U. B., Sinha, M. K., Gingerich, R. L., Scherer, P. E., and Ahima, R. S. (2004) Regulation of resistin expression and circulating levels in obesity, diabetes, and fasting. *Diabetes* **53,** 1671–1679
26. Ellis, J. M., Mentock, S. M., Depetrillo, M. A., Koves, T. R., Sen, S., Watkins, S. M., Muoio, D. M., Cline, G. W., Taegtmeyer, H., Shulman, G. I., Willis, M. S., and Coleman, R. A. (2011) Mouse cardiac acyl-coenzyme A synthetase 1 deficiency impairs fatty acid oxidation and induces cardiac hypertrophy. *Mol. Cell. Biol.* **31,** 1252–1262
27. Li, L. O., Ellis, J. M., Paich, H. A., Wang, S., Gong, N., Altshuller, G., Thresher, R. J., Koves, T. R., Watkins, S. M., Muoio, D. M., Cline, G. W., Shulman, G. I., and Coleman, R. A. (2009) Liver-specific loss of long chain acyl-CoA synthetase-1 decreases triacylglycerol synthesis and β-oxidation and alters phospholipid fatty acid composition. *J. Biol. Chem.* **284,** 27816–27826
28. Reaven, P., Merat, S., Casanada, F., Sutphin, M., and Palinski, W. (1997) Effect of streptozotocin-induced hyperglycemia on lipid profiles, formation of advanced glycation end products in lesions, and extent of atherosclerosis in LDL receptor-deficient mice. *Arterioscler. Thromb. Vasc. Biol.* **17,** 2250–2256
29. Naggert, J., Svenson, K. L., Smith, R. V., Paigen, B., and Peters, L. L. (2012) *Diet Effects on Bone Density and Content, Body Composition, and Plasma Glucose, Leptin, and Insulin Levels in 43 Inbred Strains of Mice on a High Fat Atherogenic Site.* The Jackson Laboratory, Bar Harbor, ME
30. Le Lay, J., Tuteja, G., White, P., Dhir, R., Ahima, R., and Kaestner, K. H. (2009) CRTC2 (TORC2) contributes to the transcriptional response to fasting in the liver but is not required for the maintenance of glucose homeostasis. *Cell Metab.* **10,** 55–62
31. Loncar, D. (1991) Convertible adipose tissue in mice. *Cell Tissue Res.* **266,** 149–161
32. Ortega, F. J., Moreno-Navarrete, J. M., Ribas, V., Esteve, E., Rodriguez-Hermosa, J. I., Ruiz, B., Peral, B., Ricart, W., Zorzano, A., and Fernández-Real, J. M. (2009) Subcutaneous fat shows higher thyroid hormone receptor-alpha1 gene expression than omental fat. *Obesity* **17,** 2134–2141
33. Rossmeisl, M., Barbatelli, G., Flachs, P., Brauner, P., Zingaretti, M. C., Marelli, M., Janovská, P., Horáková, M., Syrový, I., Cinti, S., and Kopecký, J. (2002) Expression of the uncoupling protein 1 from the *aP2* gene promoter stimulates mitochondrial biogenesis in unilocular adipocytes *in vivo*. *Eur. J. Biochem.* **269,** 19–28
34. Kopecky, J., Clarke, G., Enerbäck, S., Spiegelman, B., and Kozak, L. P. (1995) Expression of the mitochondrial uncoupling protein gene from the *aP2* gene promoter prevents genetic obesity. *J. Clin. Invest.* **96,** 2914–2923
35. Lefebvre, A. M., Laville, M., Vega, N., Riou, J. P., van Gaal, L., Auwerx, J., and Vidal, H. (1998) Depot-specific differences in adipose tissue gene expression in lean and obese subjects. *Diabetes* **47,** 98–103
36. Sewter, C. P., Blows, F., Vidal-Puig, A., and O'Rahilly, S. (2002) Regional differences in the response of human pre-adipocytes to PPARγ and RXRα agonists. *Diabetes* **51,** 718–723
37. Adams, M., Montague, C. T., Prins, J. B., Holder, J. C., Smith, S. A., Sanders, L., Digby, J. E., Sewter, C. P., Lazar, M. A., Chatterjee, V. K., and

O'Rahilly, S. (1997) Activators of peroxisome proliferator-activated receptor γ have depot-specific effects on human preadipocyte differentiation. *J. Clin. Invest.* **100,** 3149–3153
38. Tran, T. T., Yamamoto, Y., Gesta, S., and Kahn, C. R. (2008) Beneficial effects of subcutaneous fat transplantation on metabolism. *Cell Metab.* **7,** 410–420
39. Flachs, P., Novotný, J., Baumruk, F., Bardová, K., Bourová, L., Miksík, I., Sponarová, J., Svoboda, P., and Kopecký, J. (2002) Impaired noradrenaline-induced lipolysis in white fat of aP2-Ucp1 transgenic mice is associated with changes in G-protein levels. *Biochem. J.* **364,** 369–376
40. Li, K., Li, L., Yang, M., Liu, H., Boden, G., and Yang, G. (2012) The effects of fibroblast growth factor-21 knockdown and overexpression on its signaling pathway and glucose-lipid metabolism *in vitro*. *Mol. Cell. Endocrinol.* **348,** 21–26
41. Kharitonenkov, A., Shiyanova, T. L., Koester, A., Ford, A. M., Micanovic, R., Galbreath, E. J., Sandusky, G. E., Hammond, L. J., Moyers, J. S., Owens, R. A., Gromada, J., Brozinick, J. T., Hawkins, E. D., Wroblewski, V. J., Li, D. S., Mehrbod, F., Jaskunas, S. R., and Shanafelt, A. B. (2005) FGF-21 as a novel metabolic regulator. *J. Clin. Invest.* **115,** 1627–1635
42. Coskun, T., Bina, H. A., Schneider, M. A., Dunbar, J. D., Hu, C. C., Chen, Y., Moller, D. E., and Kharitonenkov, A. (2008) Fibroblast growth factor 21 corrects obesity in mice. *Endocrinology* **149,** 6018–6027
43. Xu, J., Lloyd, D. J., Hale, C., Stanislaus, S., Chen, M., Sivits, G., Vonderfecht, S., Hecht, R., Li, Y. S., Lindberg, R. A., Chen, J. L., Jung, D. Y., Zhang, Z., Ko, H. J., Kim, J. K., and Véniant, M. M. (2009) Fibroblast growth factor 21 reverses hepatic steatosis, increases energy expenditure, and improves insulin sensitivity in diet-induced obese mice. *Diabetes* **58,** 250–259
44. Gullberg, H., Rudling, M., Forrest, D., Angelin, B., and Vennström, B. (2000) Thyroid hormone receptor β-deficient mice show complete loss of the normal cholesterol 7α-hydroxylase (CYP7A) response to thyroid hormone but display enhanced resistance to dietary cholesterol. *Mol. Endocrinol.* **14,** 1739–1749
45. Gullberg, H., Rudling, M., Saltó, C., Forrest, D., Angelin, B., and Vennström, B. (2002) Requirement for thyroid hormone receptor β in T_3 regulation of cholesterol metabolism in mice. *Mol. Endocrinol.* **16,** 1767–1777
46. Shin, D. J., Plateroti, M., Samarut, J., and Osborne, T. F. (2006) Two uniquely arranged thyroid hormone-response elements in the far upstream 5′-flanking region confer direct thyroid hormone regulation to the murine cholesterol 7α-hydroxylase gene. *Nucleic Acids Res.* **34,** 3853–3861
47. Adams, A. C., Astapova, I., Fisher, F. M., Badman, M. K., Kurgansky, K. E., Flier, J. S., Hollenberg, A. N., and Maratos-Flier, E. (2010) Thyroid hormone regulates hepatic expression of fibroblast growth factor 21 in a PPARα-dependent manner. *J. Biol. Chem.* **285,** 14078–14082
48. Dasarathy, S., Yang, Y., McCullough, A. J., Marczewski, S., Bennett, C., and Kalhan, S. C. (2011) Elevated hepatic fatty acid oxidation, high plasma fibroblast growth factor 21, and fasting bile acids in nonalcoholic steatohepatitis. *Eur. J. Gastroenterol. Hepatol.* **23,** 382–388
49. Rizki, G., Arnaboldi, L., Gabrielli, B., Yan, J., Lee, G. S., Ng, R. K., Turner, S. M., Badger, T. M., Pitas, R. E., and Maher, J. J. (2006) Mice fed a lipogenic methionine-choline-deficient diet develop hypermetabolism coincident with hepatic suppression of SCD-1. *J. Lipid Res.* **47,** 2280–2290
50. Raubenheimer, P. J., Nyirenda, M. J., and Walker, B. R. (2006) A choline-deficient diet exacerbates fatty liver but attenuates insulin resistance and glucose intolerance in mice fed a high fat diet. *Diabetes* **55,** 2015–2020
51. Jacobs, R. L., Zhao, Y., Koonen, D. P., Sletten, T., Su, B., Lingrell, S., Cao, G., Peake, D. A., Kuo, M. S., Proctor, S. D., Kennedy, B. P., Dyck, J. R., and Vance, D. E. (2010) Impaired *de novo* choline synthesis explains why phosphatidylethanolamine *N*-methyltransferase-deficient mice are protected from diet-induced obesity. *J. Biol. Chem.* **285,** 22403–22413
52. Wang, Y. Z., and Xu, Z. R. (1999) Effect of feeding betaine on weight gain and carcass trait of barrows and gilts and approach to mechanism. *J. Zhejiang Agric. Univ.* **25,** 281–285
53. Xu, Z., Wang, M., and Huai, M. (1999) The approach of the mechanism of growth-promoting effect of betaine on swine. *Chin. J. Vet. Sci.* **19,** 399
54. Xu, Z., and Zhan, X. (1998) Effects of betaine on methionine and adipose metabolism in broiler chicks. *Acta Vet. Zoot. Sinica* **29,** 212–219
55. Yu, D., Feng, J., and Xu, Z. (2001) Effects of betaine on fat and protein metabolism in different stages of swine. *Chin. J. Vet. Sci.* **21,** 200–203
56. Yu, D. Y., and Xu, Z. R. (2000) Effects of methyl donor on the performances and mechanisms of growth-promoting hormone in piglets. *Chin. J. Anim. Sci.* **36,** 8–10
57. Wang, Y. Z., Xu, Z. R., and Chen M. L. (2000) Effects of betaine on carcass fat metabolism of meat duck. *Chin. J. Vet. Sci.* **20,** 409–413
58. Zou, X. T. (2001) Effects of betaine on endocrinology of laying hens and its mechanism of action. *Chin. J. Vet. Sci.* **21,** 300–303
59. Zou, X. T., and Lu, J. J. (2002) Effects of betaine on the regulation of the lipid metabolism in laying hen. *Sci. China* **1,** 1043–1049
60. Zou, X. T., Ma, Y. L., and Xu, Z. R. (1998) Effects of betaine and thyroprotein on laying performance and approach to mechanism and effect in hens. *Acta Agriculturae Zhejiangensis* **10,** 144–149
61. Wang, Z., Yao, T., Pini, M., Zhou, Z., Fantuzzi, G., and Song, Z. (2010) Betaine improved adipose tissue function in mice fed a high fat diet. A mechanism for hepatoprotective effect of betaine in nonalcoholic fatty liver disease. *Am. J. Physiol. Gastrointest. Liver Physiol.* **298,** G634–G642